HDAC6/aggresome processing pathway importance for inflammasome formation is context-dependent

Longlong Wang[1],[*], Shihua Shi[1], Adeline Unterreiner[2], Ronan Kapetanovic[1], Sucheta Ghosh[1,3], Jacint Sanchez[1], Selma Aslani[2], Yuan Xiong[4,5], Chi-Lin Hsu[4,5], Katherine A. Donovan[4,5], Christopher J. Farady[2], Eric S. Fischer[4,5], Frédéric Bornancin[2], and Patrick Matthias[1,3,*]

From the [1]Friedrich Miescher Institute for Biomedical Research, Basel, Switzerland; [2]Novartis Institutes for Biomedical Research, Basel, Switzerland; [3]Faculty of Sciences, University of Basel, Basel, Switzerland; [4]Department of Cancer Biology, Dana Farber Cancer Institute, Boston, Massachusetts, USA; [5]Department of Biological Chemistry and Molecular Pharmacology, Harvard Medical School, Boston, Massachusetts, USA

Reviewed by members of the JBC Editorial Board. Edited by Clare E. Bryant

The inflammasome is a large multiprotein complex that assembles in the cell cytoplasm in response to stress or pathogenic infection. Its primary function is to defend the cell and promote the secretion of pro-inflammatory cytokines, including IL-1β and IL-18. Previous research has shown that in immortalized bone marrow-derived macrophages (iBMDMs) inflammasome assembly is dependent on the deacetylase HDAC6 and the aggresome processing pathway (APP), a cellular pathway involved in the disposal of misfolded proteins. Here we used primary BMDMs from mice in which HDAC6 is ablated or impaired and found that inflammasome activation was largely normal. We also used human peripheral blood mononuclear cells and monocyte cell lines expressing a synthetic protein blocking the HDAC6-ubiquitin interaction and impairing the APP and found that inflammasome activation was moderately affected. Finally, we used a novel HDAC6 degrader and showed that inflammasome activation was partially impaired in human macrophage cell lines with depleted HDAC6. Our results therefore show that HDAC6 importance in inflammasome activation is context-dependent.

The inflammasome is a critical protein complex involved in the body's immune response (1). When activated, the inflammasome releases the pro-inflammatory cytokines interleukin (IL)-1β and IL-18, which can result in tissue damage and cell death through pyroptosis (2). Several sensor proteins can nucleate inflammasome assembly, including NLRP and NLRC subfamilies, AIM2, and pyrin. Among these, the NLRP3 inflammasome, which is key for sterile inflammation has been extensively studied (3). Activation of the NLRP3 inflammasome often requires a transcriptional priming step to upregulate the inflammasome components such as NLRP3 and IL-1β. Priming agents, e.g., bacterial lipopolysaccharide (LPS), tumor necrosis factor (TNF), or phorbol 12-myristate 13-

acetate (PMA), also trigger critical post-translational modifications that sensitize the inflammasome components to subsequent activation. Various stimuli, including the pore-forming toxin nigericin, adenosine-triphosphate (ATP) (4), and monosodium urate crystals (MSU) (5) can stimulate NLRP3 inflammasome assembly, leading to pro-caspase one activation, followed by cleavage and release of IL-1β (3). Aberrant inflammasome activity has been linked to many diseases (3), and a detailed understanding of the inflammasome's activation process is crucial for the development of potential treatments for diseases related to inflammation and immune responses.

The aggresome processing pathway (APP) is a stress-response pathway that is activated when misfolded proteins accumulate; it promotes the formation of the aggresome, a deposit of misfolded and ubiquitinated proteins near the microtubule-organizing center (MTOC), which is subsequently eliminated by autophagy (6). An essential component of the APP is the lysine deacetylase HDAC6 (7), an atypical enzyme with two catalytic domains and a zinc finger domain (ZnF-UbP, hereafter ZnF) binding the small protein ubiquitin (Ub). HDAC6 has been implicated in diverse normal or pathological cellular processes, such as stress response (e.g., APP and stress granules formation) (8), cancer (9), inflammation, and viral infection (10). Depending on the situation, the catalytic domains (regulating acetylation levels of the relevant substrate) and/or the ZnF domain (recruiting Ub) are important for optimal HDAC6 function. In its role in the APP, HDAC6 acts as an adapter protein that promotes the transport of ubiquitinated misfolded proteins by dynein motor proteins along the MTs towards the MTOC. For this, both the ZnF and the catalytic domains are critical.

It has recently been proposed that the formation of the NLRP3 and pyrin inflammasomes takes place near the MTOC and uses components of the APP machinery and that consequently inflammasome formation is impaired in cells lacking HDAC6 or expressing HDAC6 with a mutated ZnF domain (11). Furthermore, the lysosomal Ragulator complex was recently reported to activate the NLRP3 inflammasome in vivo

* For correspondence: Longlong Wang, longlong.wang@fmi.ch; Patrick Matthias, patrick.matthias@fmi.ch.
Present address for Ronan Kapetanovic: INRAE, Université de Tours, ISP, Nouzilly, France.

via HDAC6 (12). Given the apparent similarity between inflammasome formation and APP – in both cases assembly of a complex near the MTOC – it is plausible that HDAC6 could be involved in both pathways, but to define the absolute requirement of HDAC6 in inflammasome activation, a robust profiling of orthogonal methods needs to be tested in different settings. Here we have examined the importance of HDAC6 for inflammasome activation in different cellular systems, including primary mouse cells (BMDMs), peripheral blood mononuclear cells (PBMCs), and human cell lines, and manipulated HDAC6 levels through different approaches. Under the conditions tested, we found that the activation of NLRP3 was only partially dependent on HDAC6.

Results

NLRP3 inflammasome is activated efficiently in HDAC6 KO and ZnF[m] BMDMs

Previous work identified the role of HDAC6 in inflammasome activation in immortalized bone marrow-derived macrophages (iBMDMs) (11). To avoid alterations in transcriptome and other cellular processes associated with the establishment of an immortalized cell line, we first used primary BMDMs from wild-type (WT) mice as well as two mouse lines in which HDAC6 is either ablated (KO) (13) or contains a W1116A point mutation in the ZnF domain (ZnF[m], manuscript in preparation), which abolishes ubiquitin binding (10). BMDMs of the different genotypes were first primed by LPS and then challenged by nigericin, which activates the NLRP3 inflammasome by raising intracellular potassium (K^+) efflux (14) or MSU, which leads to the generation of reactive oxygen species (ROS) through activation of NADPH oxidases (5). Inflammasome activation was monitored by examining the cleaved Caspase-1 p20 fragment by immunoblotting and by measuring the release of the cytokine IL-1β in the culture supernatant (Fig. 1A). As shown in Figure 1, B and C, the generation of Caspase-1 p20 and production of IL-1β were similar in WT, KO, and ZnF[m] cells. The inflammasome dependence of the IL-1β release was confirmed by using the specific NLRP3 inhibitor MCC950 (15). Because strong inflammasome activation eventually leads to cell membrane damage and the release of cellular contents, we examined cellular toxicity by measuring the level of lactate dehydrogenase (LDH) released from cells. Also, in this case, the differences between the genotypes were minimal and did not reach statistical significance (Fig. 1D); thus, deletion or mutation of HDAC6 in primary BMDMs does not appear to protect cells from cell death. We next examined the kinetic of IL-1β release in BMDMs of the different genotypes. Interestingly, the IL-1β amount in HDAC6 KO and ZnF[m] BMDMs reached a plateau rapidly in only 15 min after the nigericin challenge, while WT BMDMs responded to stimulation more slowly (Fig. S1). At later time points (between 30 and 90 min), the IL-1β difference between the three BMDMs types was less significant, although the ZnF[m] BMDMs showed a slightly reduced level. Collectively, our results in primary BMDMs did not demonstrate a clear dependency on HDAC6 or its ZnF domain for NLRP3 inflammasome activation but indicate that HDAC6 may participate in the early timepoint response.

A ZnF-specific DARPin moderately inhibits NLRP3 inflammasome activation in THP-1 cells

To investigate more broadly the role of the HDAC6 ZnF in NLRP3 inflammasome activation, we switched from primary BMDMs to the leukemic THP-1 monocyte/macrophage cell line, a widely used surrogate for human monocytes or macrophages. We recently reported a synthetic protein based on a designed ankyrin repeat protein (DARPin) scaffold, DARPin F10, which can selectively bind to the HDAC6 ZnF Ub binding pocket in cells and blocks Ub recruitment (16) (Fig. 2A). We previously showed that DARPin F10 is highly specific for the HDAC6 ZnF (16). We made a degradable version of DARPin F10 by fusing it to the FKBP[F36V] degron tag (15) and showed that it is efficiently degraded in A549 cells upon addition of the chemical dTAG-13 (hereafter dTAG). We used this system to generate THP-1 cells expressing DARPin F10 (F10-FKBP[F36V] THP-1 cells) and found that the protein was well-expressed and could be efficiently degraded within 6 h of dTAG addition (Fig. 2B); furthermore, expression of DARPin F10 does not alter the level of endogenous HDAC6, or of the major class I HDACs, HDAC1 and 2 (Fig. S2A). Nigericin-induced NLRP3 activation was comparable in dTAG treated parental (WT) THP-1 cells (Fig. 2C) and in control cells expressing only the FKBP[F36V] moiety (FKBP[F36V] THP-1 cells, Fig. S2B), thus excluding a possible inhibitory effect of FKBP[F36V] expression or dTAG on IL-1β release. When parental WT THP-1 cells were treated with MCC950 (17), or CGP084892, a Caspase-1 inhibitor (18), IL-1β release was strongly reduced, as expected. A modest reduction of IL-1 secretion was observed in F10-FKBP[F36V] THP-1 cells when compared to the WT THP-1 cells. Degradation of DARPin F10 by dTAG treatment led to a partial, but significant, recovery of IL-1β release (Fig. 2C). We next examined early time points - 0.5 and 1.5 h post-nigericin activation - to study the impact of DARPin F10 on the kinetic of IL-1β release. In agreement with Figure 2C, we observed again a slight increase of IL-1β at 3.5 h in dTAG-treated cells (Fig. 2D). However, a larger and significant difference was seen at 1.5 h post-activation. These data indicate that blockade of the HDAC6 ZnF domain moderately inhibits the NLRP3 inflammasome, particularly during the early phase of activation by nigericin in THP-1 cells.

HDAC6 degradation moderately inhibits NLRP3 inflammasome in PBMCs

Blocking specifically the ZnF domain in THP-1 cells by DARPin F10 showed partial inhibition of NLRP3 inflammasome activation, confirming that HDAC6 contributes to this pathway. To extend these observations in other cell settings, we next made use of a novel HDAC6 proteolysis targeting chimera (PROTAC) degrader, XY-07-35 (19). Treatment of cells with XY-07-35 leads to recruitment of the E3 ligase cereblon (CRBN) to HDAC6, ubiquitination, and subsequent proteasomal degradation of HDAC6 (Fig. 3A). This degrader is based on the HDAC inhibitor suberoylanilide hydroxamic
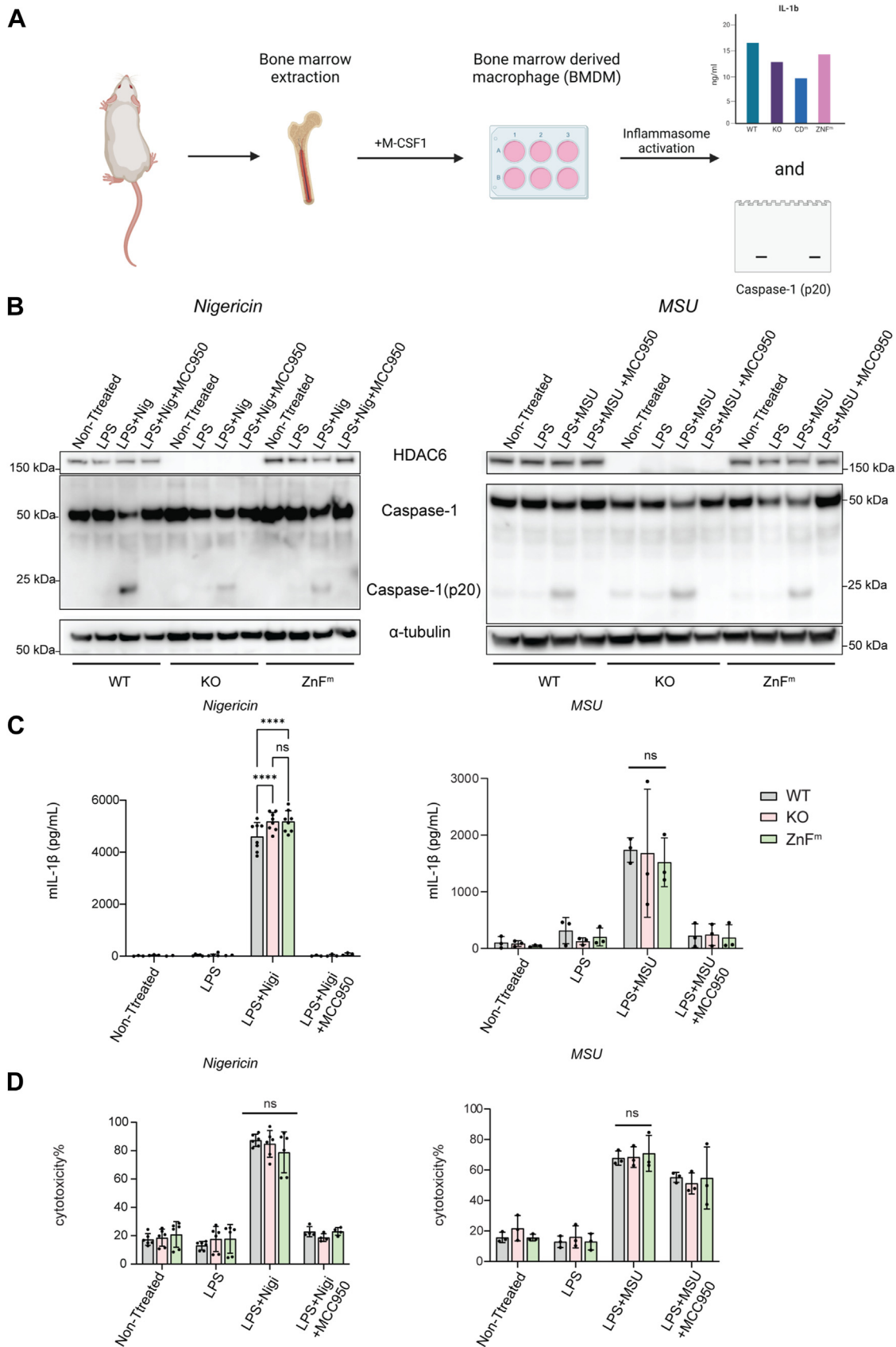
Figure 1. The NLRP3 inflammasome is activated normally in HDAC6 KO or ZnF^m primary mouse BMDMs. *A*, workflow for evaluating NLRP3 inflammasome activation in BMDMs. Bone marrow was isolated from mice strains with different mutations in HDAC6 as indicated and BMDMs were expanded for 7 days in the presence of M-CSF1. Subsequently, BMDMs were primed for 4 h with LPS (1 μg/ml) and NLRP3 inflammasome formation was induced by nigericin (20 μM) or MSU (200 μg/ml) addition. Release of IL-1β was monitored by ELISA and activation/cleavage of Caspase-1 was evaluated by
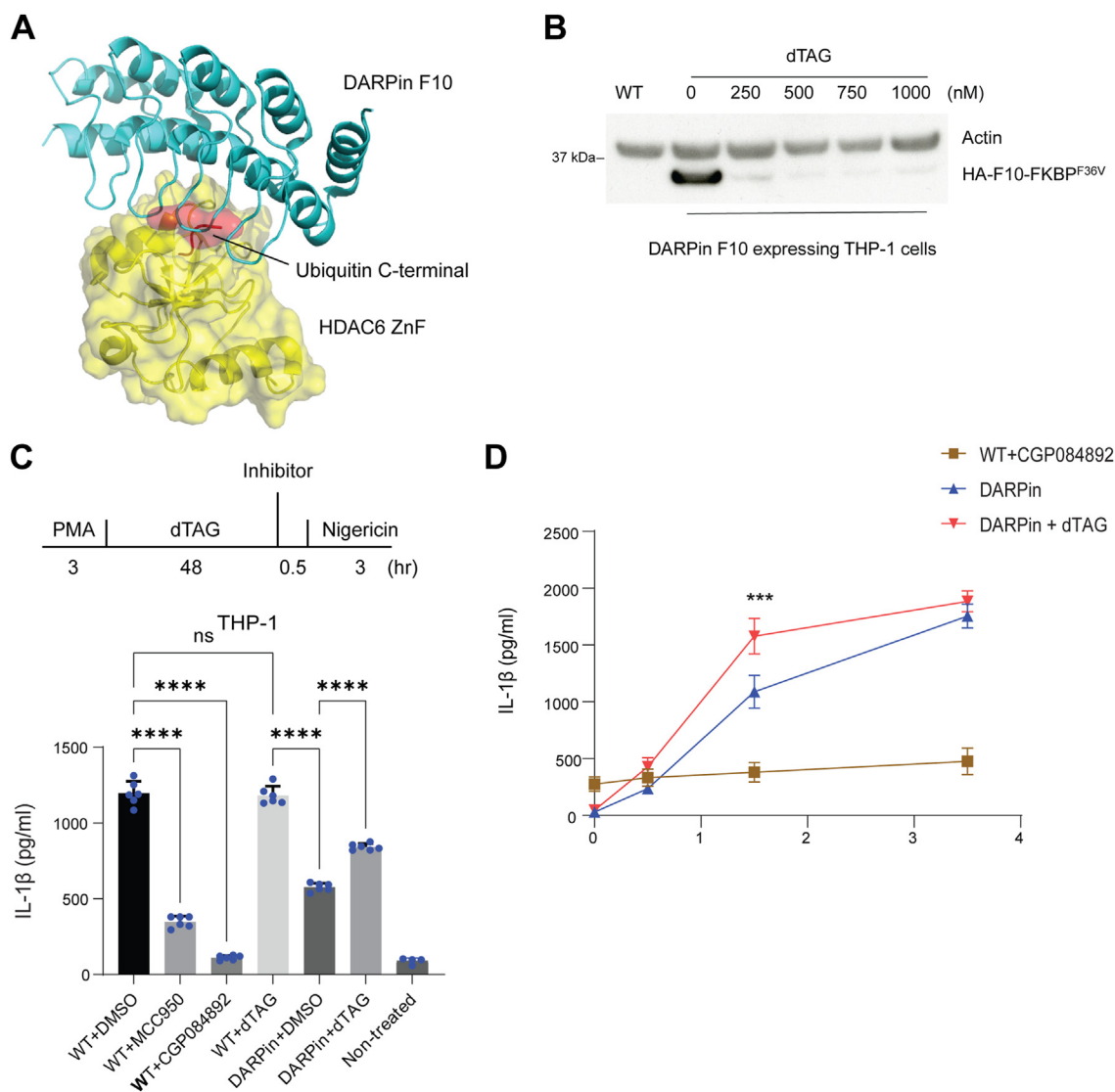
Figure 2. A DARPin blocking the HDAC6-Ub interaction has a modest effect on IL-1β release from THP-1 cells. *A*, structure of the DARPin F10 - HDAC6 ZnF domain complex (PDB: 7ZYU) showing blockade of Ub recruitment. The surface representation shows HDAC6 ZnF (*yellow*) and the C-terminal LRGG of Ub (*light pink*) (overlayed with PDB:3GV4), the ribbon representation depicts DARPIN F10 (*cyan*). *B*, establishment of a THP-1 F10-FKBP cell line with degradable DARPin F10. Immunoblotting with lysates of THP-1 F10-FKBP cells treated at the indicated concentration with dTAG (for 6 h). The leftmost lane (WT) shows the parental THP-1 cells. The membrane was probed with antibodies against actin as loading control and F10 (HA-F10-FKBP ^{F36V}, detected with anti-HA). *C*, IL-1β release under various treatments in THP-1 F10-FKBP cells at 3 h post-nigericin stimulation. Cells were treated as indicated in the scheme at the *top*. The graph at the *bottom* shows the measurement of IL-1β in cell supernatants, based on three independent experiments. MCC950 and CGP084892 are NLRP3 and Caspase-1 inhibitors, respectively. One-way ANOVA test was applied for statistical analysis. ****$p < 0.0001$. Cells were first treated with PMA (0.5 μM) for 3 h, then medium was exchanged and dTAG was added (1 μM); MCC950 (10 μM) and CGP084892 were added 30 min before nigericin (15 μM) treatment. *D*, IL-1β release from 0 h to 3.5 h after nigericin treatment in THP-1 or THP-1-F10-FKBP cells. Experimental set-up was as in (*B*) and IL-1β concentration was monitored at timepoint 0, 0.5, 1.5, and 3.5 h post nigericin treatment. Two-way ANOVA tests were applied, and comparison was performed within each timepoint between with and without dTAG group. **$p < 0.01$. Experimental setup as in (*C*).

acid (SAHA) fused by a linker to pomalidomide as a CRBN-binding moiety; the negative control compound XY-07-191 contains a methyl group on the pomalidomide moiety which disrupts CRBN recruitment (Fig. 3*B*). *In vitro* enzymatic assays with purified HDACs showed that XY-07-35 inhibited HDAC6 with a low $IC_{50} = 0.0485$ μM, which is ten times lower than for HDAC8 (0.621 μM) or other

HDACs (1.04–5.75 μM; Fig. 3*C*); in addition, the degradation profile of XY-07 to 35 is highly specific for HDAC6 (19). This compound does not show cellular toxicity when tested over a broad concentration range in either HEK293T, Jurkat or U937 cells (Fig. S3*A*).

We first tested the efficacy of XY-07-35 in immune cell lines. Unexpectedly, XY-07-35 treatment did not lead to HDAC6

immunoblotting. *B*, normal NLRP3 activation in WT, HDAC6 KO and HDAC6 ZnF^m BMDMs. Immunoblot monitoring HDAC6, Capase-1 (p20) cleavage and α-tubulin as loading control. Nigericin and MSU were used with LPS primed BMDMs (n = 3). *C*, normal mIL-1β release in the supernatant from WT, HDAC6 KO and ZnF^m BMDMs. IL-1β from supernatant in (*B*) was measured by ELISA and statistical analysis was done with one-way ANOVA. ns, no significant difference. *D*, no difference in cytotoxicity following inflammasome induction in WT, HDAC6 KO and ZnF^m BMDMs. Lactate dehydrogenase (LDH) was measured in the culture supernatant from (*B*) and statistical analysis was done by one-way ANOVA. ns, no significant difference.
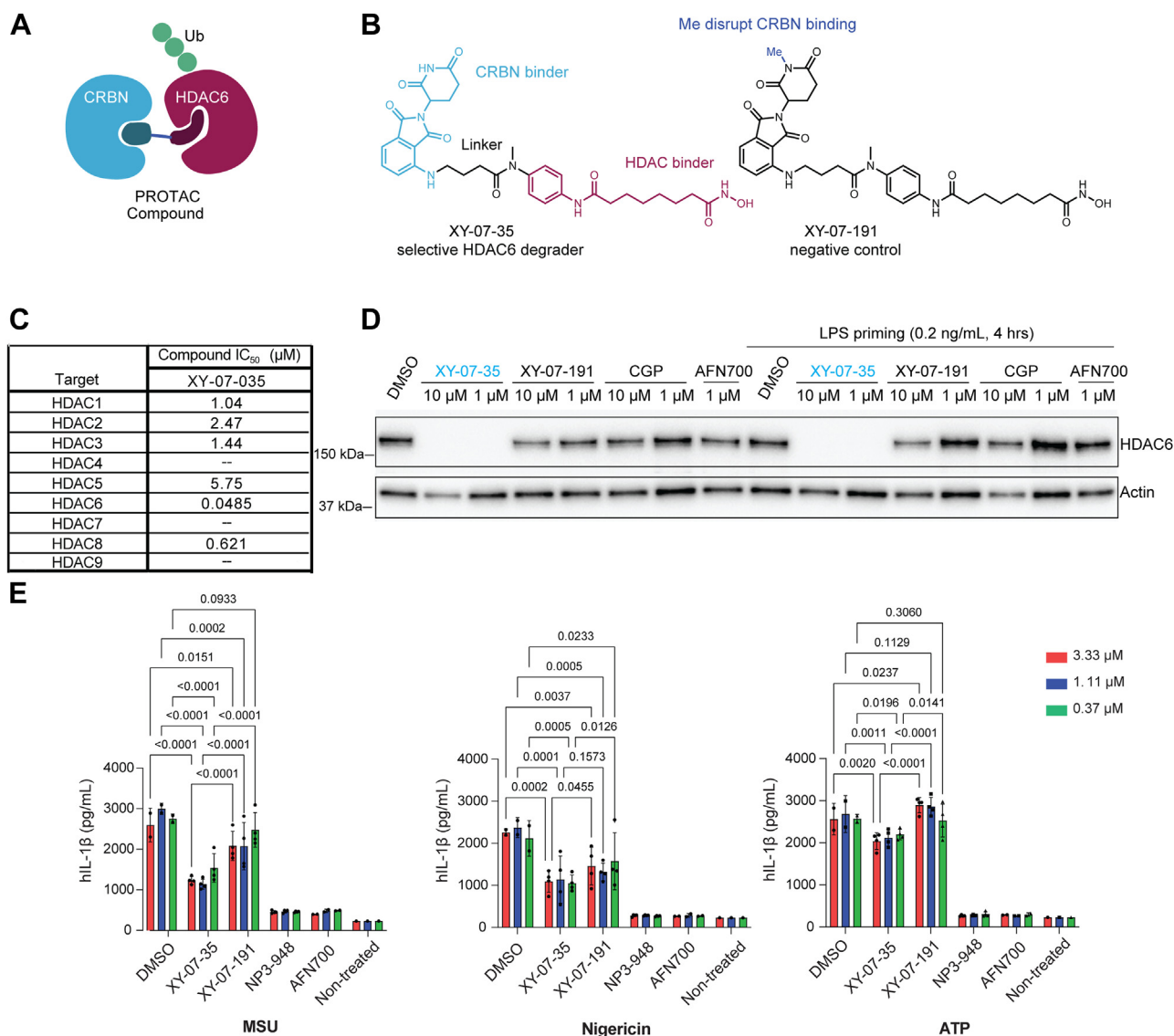
Figure 3. Effect of XY-07 to 35 mediated HDAC6 degradation on NLRP3 inflammasome activation in PBMCs. *A*, schematic of the mode of action of an HDAC6 degrader. The PROTAC engages both HDAC6 and the E3 ligase cereblon (CRBN), which then leads to ubiquitination and degradation of HDAC6. *B*, chemical structure of the HDAC6 degrader XY-07-35 and of the negative control XY-07-191 which no longer recruits CRBN. *C*, *in vitro* enzymatic assay of compound XY-07-35 on the activity of different HDACs. IC_{50} for each enzyme is shown. *D*, XY-07-35 mediated HDAC6 degradation in PBMCs. PBMCs (without or with LPS priming for 4 h) were treated with the indicated compounds and HDAC6 levels were detected by immunoblotting with an anti-HDAC6 antibody. Detection of actin was used as a control for loading. CGP, CGP084892 (Caspase-1 inhibitor); AFN700 is an inhibitor of the NF-kB pathway (IKK inhibitor). *E*, HDAC6 degradation impact on IL-1β release in PBMCs following MSU 200 μg/ml (5 h), nigericin 2 μM (2 h) or ATP 3 mM (0.5 h) treatment. Cells were first primed with 0.2 ng/ml LPS for 4 h at 37 °C, then treated with MSU, nigericin, and ATP as indicated. The graphs below show the results of three independent experiments using the inducers as indicated. NP3-948 is an inhibitor of the NLRP3 inflammasome.

degradation in both non-differentiated and PMA-differentiated THP-1 cells (Fig. S3*B*). Therefore, to assess its effect on NLRP3 inflammasome activation in human cells we used peripheral blood mononuclear cells (PBMCs). HDAC6 was efficiently degraded in PBMCs at 1 μM XY-07-35 concentration; by contrast, the negative control compound XY-07-191 or the IκKβ inhibitor AFN700 (18) had only minimal or no effect on HDAC6 levels (Fig. 3*D*). To test the functional consequence of HDAC6 degraders, PBMCs were first treated with the HDAC6 degrader or the negative control compound for 24 h, followed by LPS priming and subsequent stimulation with MSU, nigericin, or ATP to activate the NLRP3 inflammasome (Fig. 3*E*). The HDAC6 degrader XY-07-35 clearly reduced the IL-1β release

under all stimulatory conditions as compared to DMSO, though partial inhibition was also seen with the negative control XY-07-191, suggesting some non-specific effects of the scaffold. HDAC6 degradation had the most profound inhibition of MSU-triggered IL-1β release, achieving ca. 60% of IL-1β reduction as compared to DMSO, while under nigericin and ATP stimulation, the reduction was 40%. A statistically significant reduction of IL-1 between XY-07-35 and the control compound XY-07-191, was only seen in the MSU conditions. Inhibitors of other nodes of the pathway, the NLRP3 inflammasome inhibitor NP3-948 and AFN700 both led to an almost complete (>90%) inhibition of IL-1β release. The negative control compound XY-07-191 also minimally inhibited IL-1β release, but less effectively

than XY-07-35, suggesting a beneficial effect of HDAC6 degradation. We also measured cell viability by using resazurin fluorescence in PBMCs, but since monocytes constitute only a minor fraction of the cell population, the pyroptosis could not be tracked efficiently. Overall, these results show a partial reduction in NLRP3 inflammasome activation following the degradation of HDAC6, with the magnitude of the effect depending on the stimulus.

HDAC6 degradation does not affect pyrin inflammasome activation

According to a previous report (11), activation of both NLRP3 and pyrin inflammasomes depends on HDAC6. To evaluate the importance of HDAC6 for the pyrin inflammasome, we used a previously established U937 pyrin-overexpressing cell line (20). In these cells, treatment with the bile acid derivative BAA473 activates the pyrin inflammasome, leading to the release of cytokines (*e.g.*, IL-1β, IL-18) and pyroptosis; IL-18 expression is induced without the need for prior priming and was used for monitoring inflammasome activation. HDAC6 was efficiently degraded in the U937-pyrin-expressing cells by XY-07-35 at concentrations ranging from 0.1 μM to 10 μM (Fig. 4*A*). However, treatment with XY-07-35 did not result in any change in IL-18 secretion compared to either the DMSO control or the XY-07-191 control (Fig. 4*B*).

Figure 4. Effect of HDAC6 degradation on pyrin inflammasome activation in U937 cells. *A*, XY-07-35 mediated HDAC6 degradation in pyrin-expressing U937 cells. Cells were treated with the indicated compounds and HDAC6 was detected by immunoblotting with an anti-HDAC6 antibody. Detection of actin was used as a control for protein loading. *B*, no impact of HDAC6 degradation on IL-18 release in U937-pyrin cells treated with the indicated compounds. Pyrin inflammasome was activated by BAA473 (200 μM) for 4 h at 37 °C. The scheme at the *top* depicts the experimental outline. The graph at the *bottom* presents IL-18 release based on four independent experiments. CGP, CGP084892 (200 μM). ns, no significant difference.

Additionally, we measured cell viability and found that HDAC6 degradation by XY-07-35 did not protect cells from pyroptosis (Fig. S4), confirming that in this setting, HDAC6 degradation has no effect on pyrin inflammasome activation.

Discussion

In this study, we utilized a range of cellular systems and several orthogonal approaches to modulate HDAC6 activity and probe its role in NLRP3 and pyrin inflammasome activation. HDAC6 protein levels were modulated by both knockout and chemically induced degradation, while the function was probed by a knock-in unable to bind to ubiquitin and a DARPin inhibitor blocking ubiquitin recruitment. In contrast to a previous study reporting on the HDAC6-ubiquitin interaction as a crucial regulator of inflammasome activation (11), we did not observe a significant difference in NLRP3 inflammasome activation between WT and HDAC6 knock-out or HDAC6 ZnF^m (W1116A) BMDM cells. To investigate this further, we examined the effect of a small protein (DARPin F10) binding to the HDAC6 ZnF domain and preventing ubiquitin recruitment. This protein was shown to have a strong inhibitory impact on processes involving the ZnF-Ub interaction, such as the formation of aggresomes or stress granules, or infection by influenza or Zika virus (16). However under conditions of inflammasome induction, we observed only partial downregulation of IL-1β release in THP-1 cells expressing DARPin F10 when stimulated with nigericin. In primary PBMCs and U937 cells, the selective HDAC6 degrader XY-07-35 efficiently degraded HDAC6, but HDAC6 had only modest, stimulation-dependent effects on NLRP3 inflammasome activation. Furthermore, HDAC6 degradation had no effect on IL-18 release and pyroptosis mediated by pyrin. With respect to NLRP3 inflammasome activation, HDAC6 degradation had the strongest effect on MSU-stimulated IL-1β release, which is a milder, non-pyroptotic form of NLRP3 activation (Fig. 3*E*). Similarly, in THP1 cells, HDAC6 inhibition seemed to have its most pronounced effect at early timepoints. It is possible that HDAC6 plays a more pronounced role in response to crystalline inflammasome activators (in agreement with the results of Magupali *et al.*, 2022). It has also been noted that other NLRP3 regulatory mechanisms such as PKD phosphorylation play an important role at early time points in cell culture experiments, but compensatory pathways override these effects at later timepoints (21).

Based on our results it seems that the importance of HDAC6 for NLRP3 inflammasome activation is not absolute, but condition and context-dependent. On one hand, we noted that blocking the HDAC6 ZnF-Ub interaction with DARPin F10 in THP-1 cells and degrading HDAC6 in PBMCs both resulted in an inhibitory effect, thus supporting a role for HDAC6 in this pathway. When degrading DARPin F10 with dTAG we only observed a partial rescue of IL-1β release; this can possibly be explained by incomplete degradation of DARPin F10, leading to some residual F10 (even in tiny amounts) that could interfere with ubiquitin recruitment. Similarly, incomplete HDAC6 clearance by the proteasome system might be responsible for the moderate downregulation of IL-1β release or cell death protection in XY-

07-35 treated PBMCs. Furthermore, we found that the negative control compound XY-07-191 also exhibited slight inhibition of NLRP3 inflammasome activation, which we attribute to its possible catalytic inhibition of HDAC6. Indeed, both compounds are derived from SAHA (Fig. 3B), which is known to inhibit all HDACs including HDAC6, and previous studies have demonstrated that HDAC inhibition can downregulate IL-1β release (11, 22). Context dependence for HDAC6 inflammasome activation has also been observed in HDAC6 inhibitor studies. For instance, a recent study in THP-1 cells (23) showed that inhibiting HDAC6 by Tubastatin A leads to a reduced IL-1β release, but in another study in BMDMs (24), Tubastatin A did not impact the mIL-1β level. We notice these differences and remark that current HDAC inhibitors, including HDAC6-selective inhibitors, may not be as specific as previously reported (25).

On the other hand, we found that the activation of the NLRP3 inflammasome in BMDMs from HDAC6 KO and ZnF^{m} (W1116A) mice took place normally; likewise, activation of the pyrin inflammasome in U937-pyrin cells was not affected by HDAC6 depletion. In a previous study using immortalized BMDMs (11), researchers described an HDAC6-mediated aggresome-like pathway for NLRP3 inflammasome formation and reported that deletion of HDAC6 or mutations in the ZnF domain completely blocked inflammasome activation, in contrast to our results. Likewise, another recent study reported that the lysosomal Ragulator complex is important for NLRP3 inflammasome activation *in vivo* via interaction with HDAC6 (12).

We hypothesize that the partial discrepancy may result from the differences in the cell types and specific experimental conditions used. Immortalized cells are known to carry chromosomal abnormalities that allow them to proliferate indefinitely, leading to changes in their transcriptome, proteome, and reliance on specific pathways compared to primary cells. As a result, it is reasonable to speculate that established iBMDMs may behave differently from primary BMDMs. As for the pyrin inflammasome, we used U937 cells instead of iBMDMs, and bile acid derivatives instead of Clostridioides difficile toxin B (TcdB) to activate the pathway, which may also contribute to the observed differences in results obtained. In summary, we conclude that HDAC6 can participate in NLRP3 inflammasome activation, but its importance appears to be context dependent.

Experimental procedures

Cell culture

THP-1, U937, PBMC, and BMDM cells were cultured in Roswell Park Memorial Institute (RPMI) 1640 Medium–stable Glutamine (Bioconcept#1-41F03-1) supplemented with 10% fetal bovine serum (FBS). For BMDMs, the medium also contained M-CSF 1 (100 ng/ml). All cells were cultured in 5% CO_2 at 37 °C.

BMDMs isolation and culture

BMDMs were isolated as previously described (26). In short, mice (8~14 weeks old) were sacrificed and both legs were sterilized in 70% ethanol. The attached tissues were removed by dissection with scissors and the isolated bones were flushed or crushed twice in a mortar with 5 ml RPMI 1640 medium. The suspension from crushed bones was filtered through 100 μm cell strainer (Falcon#352360) to remove debris. Filtered cells were centrifuged at 500g, 15 min at room temperature. The supernatant was removed and cell pellets were resuspended in RPMI 1640 (+M-CSF 1, 100 ng/ml). The cell suspension (from one leg) was divided into four Nunc Square 25-cm dishes (Thermo Scientific#166508), with each plate containing 10 ml cell suspension. On Day 3 post-seeding, 5 ml fresh RPMI 1640 (+M-CSF 1) medium was added to each plate. On Day 6, BMDMs were ready for collection or re-seeding for new experiments. All mice handling was done according to Swiss federal guidelines for animal experimentation and approved by the FMI Animal Committee and the local veterinary authorities (Kantonales Veterinäramt of Kanton Basel-Stadt).

Immunoblotting

Treated BMDM cells were lysed with RIPA buffer (supplied with cOmplete Protease Inhibitor Cocktail, Merck# 11697498001), and protein concentration was determined by Bradford assay. The same protein amounts were loaded onto 4 to 12% NuPAGE Gels and protein was transferred to PVDF membranes by using Trans-Blot Turbo Transfer System (Biorad#17001917). The membrane was blocked with 5% milk-TBS, and then incubated with primary antibodies overnight at 4 °C. The signal was developed with HRP-conjugated secondary antibodies and Amersham ECL Western Blotting Detection Reagent (Cytiva#RPN2106). Antibody information: mouse Caspase-1 (p20) (AdipoGen#AG-20B-0042-C100), mHDAC6 (homemade), human HDAC6 (CellSignaling#7558), α-tubulin (Sigma-Aldrich #T9026), HA (CellSignaling#3724), pan Actin (Sigma-Aldrich#SAB4502632).

ELISA (for IL-1β and IL-18)

Supernatant from treated cells were collected and frozen at −80 °C before determining cytokine concentrations. mIL-1β was determined by ELISA MAX Standard Set Mouse IL-1β kit (BioLegend# 432601). Human IL-1β and IL-18 were determined with Cisbio HTRF Cisbio Human IL1β (#62HIL1BPET) and Human IL18 (#62HIL18PEG) protocols. All the data were from 3 or 4 independent biological replicates.

LDH measurement

Culture supernatants from the different BMDM samples were analyzed with the CytoTox 96 Non-Radioactive Cytotoxicity Assay Kit (Promega# G1780). Total cell lysate of non-treated (*i.e.*, DMSO only -no inhibitor-, but induced for inflammasome formation) BMDM cells was defined as 100% cell death or cytotoxicity. Values from other conditions were calculated as follows: $(OD_{treated\ cells} - OD_{no\text{-}inhibitor}\ control) \div (OD_{total\ lysate} - OD_{no\text{-}inhibitor\ control}) * 100$.

𝒮ASBMB

J. Biol. Chem. (2024) 300(2) 105638 **7**

HDAC6 and inflammasome activation

Single-cell clonal THP-1 F10 and FKBP cells establishment

Lentiviral vectors for HA-DARPin F10-FKBP[F36V] and HA-FKBP[F36V] were from previous work ([16]). Lentivirus was generated with third-generation lentivirus packaging systems. In detail, DARPin F10 vector and lentivirus packaging plasmids (Tat, Rev, Gag/pol, Vsv-g) were co-transfected in 293T cells in six well-plates. After 3 days of culturing, supernatants were harvested and concentrated with Lenti-X Concentrator (Takara# 631232). The virus pellet was resuspended in 1∼4 ml RPMI1640 medium (with 10% FBS). Next, THP-1 cells were seeded in six-well plates (each well with 1×10^6 cells), and then lentivirus was added to the plate in the presence of polybrene (8 μg/ml), followed by centrifugation at 1500 rpm/453g, for 45 min at room T°. After transduction, THP-1 cells were cultured at 37 °C for 7∼14 days. The cell number and density were monitored carefully; when a concentration of $>2 \times 10^6$ cells per ml was reached, 2 μg/ml puromycin was added for selection for 3∼6 days. Surviving cells were single cells sorted by FACS into 96 well plates (in RPMI1640 without puromycin). After about 1 month in culture, single-cell clones were analyzed by immunoblotting to test for DARPin F10 expression. Cell clones with a good expression level were stored in cryo-solution (90% FBS + 10% DMSO) in liquid nitrogen.

Inflammasome activation

For BMDM cells, 1.5×10^6 cells per well were seeded in six-well plates. After priming with 1 μg/ml LPS (Invivogen #tlrl-b5lps), cells were challenged with 200 μg/ml MSU crystals (Invivogen #tlrl-msu-25) for 6 h or 20 μM nigericin (Sigma-Aldrich #N7143-5MG) for 30 min. For THP-1 cells, 5×10^5 cells/ml were primed with 0.5 μM PMA (Invivogen #tlrl-pma) in T75 Ultra-low binding flask (CORNING #3814) for 3 h, and then cells were collected by centrifugation at 500g, for 5 min. The supernatant was removed, and fresh medium was added to have cells at a density of around 5×10^5 cells/ml. 100 μl cells were seeded in 96-well plate and incubated for 1∼2 days. During the culturing, dTAG was added when needed to degrade the DARPin. After 1∼2 days of culturing, inflammasome was activated by adding 15 μM nigericin for up to 4 h. For PBMCs, 3×10^4 cells per were seeded, and primed with 0.2 ng/ml LPS for 4 h and then incubated with MSU 200 μg/ml (5 h), nigericin 2 μM (2 h) or ATP 3 mM (0.5 h). For pyrin inflammasome, U937-pyrin cells were seeded in 96 well after 0.5 μM PMA treatment for 3 h and then challenged by BAA473 (200 μM) for 4 h at 37 °C. For control experiments inhibitors were used at the following final concentration: MCC950 at 10 μM, CGP084892 at 20 μM. NP3-948 is a potent NLRP3 inhibitor developed at Novartis that competes with MCC950 for binding to the NLRP3 protein ([27]).

Cell viability assay

Cell viability of PBMCs and U937 cells was checked with PrestoBlue HS Cell Viability Reagent (Invitrogen # P50200) according to the manufacturer's instructions. After incubation for 1 to 2 h, fluorescence was determined with a PheraStar plate reader under Ex/Em = 540/590 nm.

Cell viability with CTG assay

U937, Jurkat, and HEK293T cells were plated with a density of 10^5 cells/ml, with 50 μl/well in a white 384 well plate (Corning #3570). Two hours after plating, XY-07-035 was dispensed to each well using HPd300e and incubated at 37 °C for 70 h. CellTiter-Glo (CTG) Luminescent Cell Viability Assay (Promega #G7572) was then used to measure cell viability. Aliquoted frozen CTG reagent and cell plates were warmed to room temperature prior to loading. After the plates were cooled to room temperature, the CTG reagent was loaded 15 μl/well with an electronic multichannel pipette. To ensure the reagent had fully reacted with cells, plates were centrifuged at 500g, 3 min followed by a 30 min incubation in a dark box at room temperature. The luminescence signal was read over ten cycles for each data point on a PHERAstar FS microplate reader (BMG Labtech). The Relative abundance was calculated as the sum of the averages of duplicate individual 12-point dose-response data points.

Statistical analysis

All the statistical analyses were done with one-way or two-way ANOVA test, corrected for multiple comparisons using the post hoc significance Tukey test. A significance level of $p < 0.05$ was used.

Data availability

Mass spectrometry data related to HDAC6 degrader XY-07-35 and XY-07-191 are deposited to PRIDE under archive number PXD023652. The data that supports the findings described in this work are available from the corresponding author upon request.

Abbreviations—The abbreviations used are: APP, aggresome processing pathway; iBMDMs, immortalized bone marrow-derived macrophages; IL, interleukin; LPS, lipopolysaccharide; MSU, monosodium urate crystals; MTOC, microtubule-organizing center; PMA, phorbol 12-myristate 13-acetate; TNF, tumor necrosis factor.

References

1. Mariathasan, S., Newton, K., Monack, D. M., Vucic, D., French, D. M., Lee, W. P., *et al.* (2004) Differential activation of the inflammasome by caspase-1 adaptors ASC and Ipaf. *Nature* **430**, 213–218
2. Broz, P., and Dixit, V. M. (2016) Inflammasomes: mechanism of assembly, regulation and signalling. *Nat. Rev. Immunol.* **16**, 407–420
3. Swanson, K. V., Deng, M., and Ting, J. P. (2019) The NLRP3 inflammasome: molecular activation and regulation to therapeutics. *Nat. Rev. Immunol.* **19**, 477–489
4. Perregaux, D., and Gabel, C. A. (1994) Interleukin-1 beta maturation and release in response to ATP and nigericin. Evidence that potassium depletion mediated by these agents is a necessary and common feature of their activity. *J. Biol. Chem.* **269**, 15195–15203
5. Martinon, F., Pétrilli, V., Mayor, A., Tardivel, A., and Tschopp, J. (2006) Gout-associated uric acid crystals activate the NALP3 inflammasome. *Nature* **440**, 237–241
6. Jennifer, A., Johnston, C. L. W., and Kopito, R. R. (1998) Aggresomes: a cellular response to misfolded proteins. *J. Cell Biol.* **143**, 1883–1898
7. Kawaguchi, Y., Kovacs, J., McLauri, A., Vance, J., Ito, A., and Yao, T. (2003) The deacetylase HDAC6 regulates aggresome formation and cell viability in response to misfolded protein stress. *Cell* **115**, 727–738
8. Saito, M., Hess, D., Eglinger, J., Fritsch, A. W., Kreysing, M., Weinert, B. T., *et al.* (2019) Acetylation of intrinsically disordered regions regulates phase separation. *Nat. Chem. Biol.* **15**, 51–61
9. Rodriguez-Gonzalez, A., Lin, T., Ikeda, A. K., Simms-Waldrip, T., Fu, C., and Sakamoto, K. M. (2008) Role of the aggresome pathway in cancer: targeting histone deacetylase 6-dependent protein degradation. *Cancer Res.* **68**, 2557–2560
10. Indranil Banerjee, Y. M., Miyake, Y., Nobs, S. P., Schneider, C., Horvath, P., Kopf, M., *et al.* (2014) Influenza A virus uses the aggresome processing machinery for host cell entry. *Science* **346**, 473–477
11. Magupalli, V., Negro, R., Tian, Y., Hauenstein, A., Di Caprio, G., Skillern, W., *et al.* (2020) HDAC6 mediates an aggresome-like mechanism for NLRP3 and pyrin inflammasome activation. *Science* **369**, eaas8995
12. Tsujimoto, K., Jo, T., Nagira, D., Konaka, H., Park, J. H., Yoshimura, S. I., *et al.* (2023) The lysosomal ragulator complex activates NLRP3 inflammasome in vivo via HDAC6 the. *EMBO J.* **42**, e111389
13. Zhang, Y., Kwon, S., Yamaguchi, T., Cubizolles, F., Rousseaux, S., Kneissel, M., *et al.* (2008) Mice lacking histone deacetylase 6 have hyperacetylated tubulin but are viable and develop normally. *Mol. Cell. Biol.* **28**, 1688–1701
14. Muñoz-Planillo, R., Kuffa, P., Martínez-Colón, G., Smith, B. L., Rajendiran, T. M., and andNúñez, G. (2013) K$^+$ efflux is the common trigger of NLRP3 inflammasome activation by bacterial toxins and particulate matter. *Immunity* **38**, 1142–1153
15. Natsume, T., and Kanemaki, M. T. (2017) Conditional degrons for controlling protein expression at the protein level. *Annu. Rev. Genet.* **51**, 83–102
16. Wang, L., Moreira, E. A., Kempf, G., Miyake, Y., Oliveira Esteves, B. I., Fahmi, A., *et al.* (2022) Disrupting the HDAC6-ubiquitin interaction impairs infection by influenza and Zika virus and cellular stress pathways. *Cell Rep.* **39**, 110736
17. Coll, R. C., Robertson, A. A., Chae, J. J., Higgins, S. C., Muñoz-Planillo, R., Inserra, M. C., *et al.* (2015) A small-molecule inhibitor of the NLRP3 inflammasome for the treatment of inflammatory diseases. *Nat. Med.* **21**, 248–255
18. Unterreiner, A., Rubert, J., Kauffmann, M., Fruhauf, A., Heiser, D., Erbel, P., *et al.* (2021) Pharmacological inhibition of IKKβ dampens NLRP3 inflammasome activation after priming in the human myeloid cell line THP-1. *Biochem. Biophys. Res. Commun.* **545**, 177–182
19. Xiong, Y., Donovan, K. A., Eleuteri, N. A., Kirmani, N., Yue, H., Razov, A., *et al.* (2021) Chemo-proteomics exploration of HDAC degradability by small molecule degraders. *Cell Chem. Biol.* **28**, 1514–1527.e4
20. Alimov, I., Menon, S., Cochran, N., Maher, R., Wang, Q., Alford, J., *et al.* (2019) Bile acid analogues are activators of pyrin inflammasome. *J. Biol. Chem.* **294**, 3359–3366
21. Heiser, D., Rubert, J., Unterreiner, A., Maurer, C., Kamke, M., Bodendorf, U., *et al.* (2021) Evaluation of protein kinase D auto-phosphorylation as biomarker for NLRP3 inflammasome activation. *PLoS one* **16**, e0248668
22. Xu, J., Zhao, X., Jiang, X., He, L., Wu, X., Wang, J., *et al.* (2022) Tubastatin A improves post-resuscitation myocardial dysfunction by inhibiting NLRP3-mediated pyroptosis through enhancing transcription factor EB signaling. *J. Am. Heart Assoc.* **11**, e024205
23. Bockstiegel, J., Wurnig, S. L., Engelhardt, J., Enns, J., Hansen, F. K., and Weindl, G. (2023) Pharmacological inhibition of HDAC6 suppresses NLRP3 inflammasome-mediated IL-1β release. *Biochem. Pharmacol.* **215**, 115693
24. Hwang, I., Lee, E., Jeon, S.-A., and Yu, J.-W. (2015) Histone deacetylase 6 negatively regulates NLRP3 inflammasome activation. *Biochem. Biophys. Res. Commun.* **467**, 973–978
25. Lechner, S., Malgapo, M. I. P., Gratz, C., Steimbach, R. R., Baron, A., Ruther, P., *et al.* (2022) Target deconvolution of HDAC pharmacopoeia reveals MBLAC2 as common off-target. *Nat. Chem. Biol.* **18**, 812–820
26. Afroz, S. F., Condon, N. D., Sweet, M. J., and Kapetanovic, R. (2022) Quantifying regulated mitochondrial fission in macrophages. *Methods Mol. Biol.* **2523**, 281–301
27. Dekker, C., Mattes, H., Wright, M., Boettcher, A., Hinniger, A., Hughes, N., *et al.* (2021) Crystal structure of NLRP3 NACHT domain with an inhibitor defines mechanism of inflammasome inhibition. *J. Mol. Biol.* **433**, 167309

ASBMB

J. Biol. Chem. (2024) 300(2) 105638 **9**